Experimental Study on Shear Splitting Failure of Full-Scale Composite Concrete Encased Steel Beams

C. C. Weng[1]; S. I. Yen[2]; and M. H. Jiang[3]

Abstract: Presented herein is an experimental study that focuses on the shear splitting failure of composite concrete encased steel beams. Nine full-scale specimens were constructed and tested in this study. Significant horizontal cracks along the interface of steel flange and concrete, referred to as the shear splitting failure, appeared in five tested specimens. Observations from the experiments indicate that the steel flange width ratio, defined as the ratio of steel flange width to gross section width, has a dominant effect on the shear splitting failure of composite beams. The test results reveal that the shear splitting failure occurs when the steel flange width ratio of a composite beam reaches 0.67. The test results also show that the application of shear studs has a positive effect on preventing this type of failure for beams with large steel flange ratio. In addition to the experimental study, a new method for predicting the failure mode of composite beams is proposed. The proposed method gives satisfactory predictions as compared to the test results. Finally, a new equation is derived for the design of the stirrups to prevent shear splitting failure of naturally bonded composite beams.

Introduction

Many kinds of structural members depend on the natural bond or mechanical interlock between different structural materials for their strength and stiffness. Reinforced concrete, prestressed concrete, and composite construction are obvious examples. An advantageous feature of composite construction is that it involves interaction between steel and concrete elements that are, by themselves, structural members. One type of the structural members in the composite construction is the concrete encased steel beam. Encasement of a steel shape increases its stiffness, energy absorption, and drastically reduces the possibility of local buckling of the encased steel. This type of composite member has been used in Japan for more than 4 decades (Wakabayashi 1987). It also becomes increasingly popular to use the concrete encased steel members in building construction in Taiwan after the Ji-Ji earthquake in 1999. A design guide for this type of structural member can be found from the latest edition of the steel reinforced concrete (SRC) structures design standards published by Architectural Institute of Japan (AIJ 2001).

Past studies of composite concrete encased steel members have concentrated on the strength and behavior of columns or beam columns (Procter 1967; Furlong 1968; Naka et al. 1977;

Johnson and May 1978; Mirza 1989; Ricles and Paboojian 1994; El-Tawila et al. 1995; Mirza et al. 1996; Muñoz and Hsu 1997a, b; El-Tawil and Deievlein 1999). However, situations exist in composite members where shear forces need to be transferred across the interface between steel flange and concrete. It is noted that shear splitting cracks along the interface may become critical if: (1) the width of the steel flange is approaching the overall width of the composite section or (2) the amount of stirrups (shear reinforcements) or shear studs is not adequate in the composite beam.

In the United States, the design provisions of composite structural members can be found from the American Concrete Institute building code No. ACI318-99 (ACI 1999), the American Institute of Steel Construction (AISC) specification (AISC 1999), and the National Earthquake Hazards Reduction Program (NEHRP) seismic provisions (BSSC 1997). However, due to the lack of sufficient test data on the shear behavior of concrete encased steel members, it is noted that these design provisions have not included specific design guidance to avoid the possible shear splitting failure along the interface between steel flange and concrete of the composite members.

In light of the above observations, an experimental study on the mechanical behavior of concrete encased steel beams subjected to bending and shear is conducted through the tests of nine full-scale specimens. The objectives of this study are to: (1) investigate the failure modes of composite beams; (2) study the influences of steel flange width and bond condition on the strength and behavior of composite beams; (3) develop an analytical model for predicting the shear splitting failure capacity; and (4) propose a new design method to prevent shear splitting failure of composite beams.

Experimental Program

Test Specimens

In this study, nine concrete encased steel beams were tested to failure. Table 1 shows the dimensions of the test specimens. All

[1]Professor, Dept. of Civil Engineering, National Chiao Tung Univ., 1001 Ta Hsueh Rd., Hsinchu 300, Taiwan. E-mail: weng@cc.nctu.edu.tw

[2]PhD candidate, Dept. of Civil Engineering, National Chiao Tung Univ., 1001 Ta Hsueh Rd., Hsinchu 300, Taiwan.

[3]Graduate Research Assistant, Dept. of Civil Engineering, National Chiao Tung Univ., 1001 Ta Hsueh Rd., Hsinchu 300, Taiwan.

Table 1. Dimensions of Test Specimens

Specimen designation	Bond condition	Cross section $B \times D$ (mm)	Steel Shape[a] $d_s \times b_f \times t_w \times t_f$ (nm)	Spacing of stirrups, S (mm)	Detail[a] type
		Specimens with flange width ratio[b]=0.67 (b_f=200 mm)			
B1-20-S	Shear Stud	300×500	H294×200×8×12	150	A
B2-20-G	Grease				B
B3-20-N	Natural Bond				C
B4-20-N			H294×200×8×12		
B5-20-N			H294×200×6×8		
B6-20-N			H294×200×4.5×6		
		Specimens with flange width ratio=0.50 (b_f=150 mm)			
B7-15-S	Shear Stud	300×500	H300×150×6.5×12	150	A
B8-15-G	Grease				B
B9-15-N	Natural Bond				C
		Ordinary RC beam			
B10-RC	—	300×500	—	150	—

[a]Cross-section details of specimens are shown in Fig. 1.
[b]Defined as the ratio of steel flange width to gross section width.

specimens have a 3 m clear span and a rectangular section of 300×500 mm reinforced by deformed bars 19 mm in diameter deployed at four corners. Deformed bars 10 mm in diameter are used as stirrups and are all spaced every 150 mm along the span of the specimen (see Fig. 1 for cross-section details).

To evaluate the influence of steel flange width on the failure mode (shear splitting failure or flexural failure) of the composite beams, the specimens are designed and separated into two major groups as shown in Table 1: specimens with steel flange width ratio of 0.67 and specimens with steel flange width ratio of 0.5.

The "steel flange width ratio" is defined as the ratio of the steel flange width to the gross section width.

Three different bond conditions are considered between the steel shape and concrete. They are (1) specimens with shear studs of 13 mm diameter×50 mm (denoted as S) on steel flange; (2) specimens with grease (denoted as G) between steel shape and concrete; and (3) specimens with natural bond condition (denoted as N). These specimens are designed to study the influence of bond conditions on the shear and flexural behavior of the composite beams.

Table 2 shows the material properties of the test specimens. The average 28-day compressive strength of concrete is 37.4 MPa. The concrete strength for each specimen is determined in accordance with American society for testing and materials (ASTM) test method Standard C39-72 (ASTM 1991a), testing 152×305 mm cylinders on the day of each experiment. The yielding stress f_y and tensile strength f_u of the steel shape are determined according to the ASTM method for uniaxial tension testing of metallic materials Standard E8-91 (ASTM 1991b). Similarly, f_y and f_u values of the reinforcing bars and the stirrups are averages of three tests conducted on bars 241 mm in length.

Test Setup

As shown in Fig. 2, vertical load was applied monotonically at the midlength of a specimen through a displacement-controlled method and monitored by the readings from calibrated load cells.
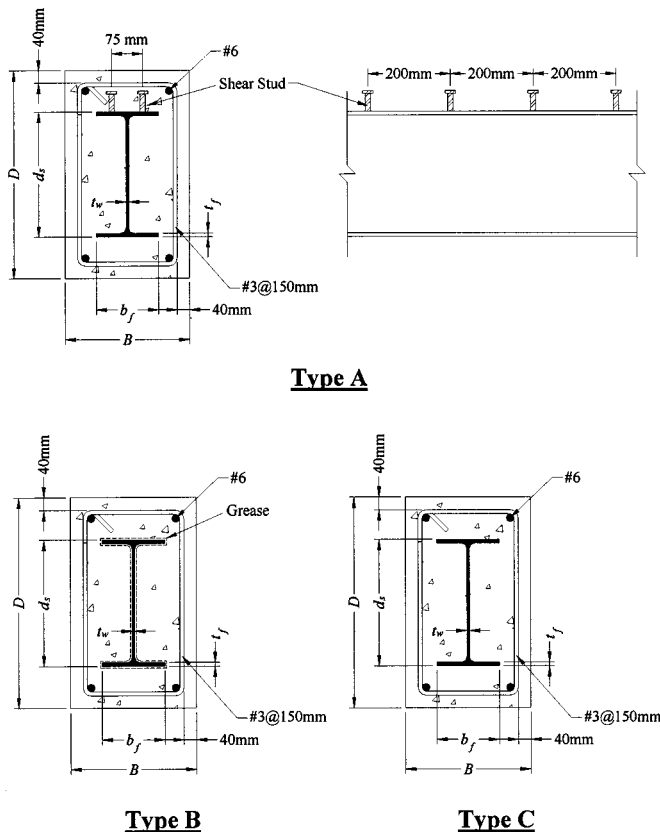

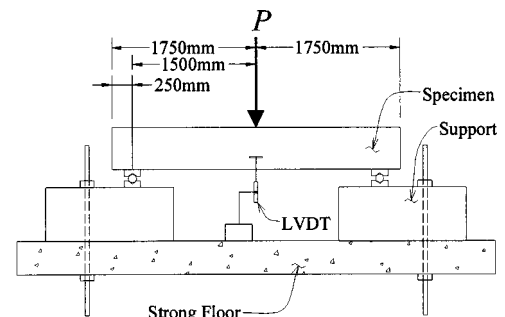**Fig. 1.** Cross-section details of test specimens

Fig. 2. Test setup

Table 2. Material Properties of Test Specimens

Specimen designation	Concrete strength f'_c (MPa)	Steel shape		Reinforcing bar		Stirrup	
		f_y (MPa)	f_u (MPa)	f_y (MPa)	f_u (MPa)	f_y (MPa)	f_u (MPa)
Specimens with flange width ratio=0.67 (b_f=200 mm)							
B1-20-S	37.4	319	445	598	716	417	578
B2-20-G	37.5	319	445	598	716	417	578
B3-20-N	37.1	319	445	598	716	417	578
B4-20-N	37.3	319	445	598	716	417	578
B5-20-N	37.8	321	449	598	716	417	578
B6-20-N	37.8	336	430	598	716	417	578
Specimens with flange width ratio=0.50 (b_f=150 mm)							
B7-15-S	37.1	367	475	598	716	417	578
B8-15-G	37.5	367	475	598	716	417	578
B9-15-N	37.8	367	475	598	716	417	578
Ordinary RC beam							
B10-RC	36.2	—	—	598	716	417	578

The control speed of the displacement was set at 0.03 mm/s. The distribution of forces within a specimen could be traced by means of electric strain gauges that were attached to the reinforcing bars and to the steel web and flanges. The transverse deflections of a specimen were measured by using the LVDT. The loads produced single curvature bending in all specimens with bending moment acting about the major axis of the steel shape.

Test Results and Discussions

Failure Modes

Based on the crack patterns observed from the tested specimens, the failure modes of the concrete encased steel beams are classified into two types. One is the ''shear splitting failure mode'' which shows horizontal cracks along the interface of steel flange and concrete; the other is the ''flexural failure mode'' which closely resembles the flexural failure of an ordinary reinforced concrete beam.

Table 3 contains a summary of the test results at failure con-

dition. This table displays the ultimate load and the corresponding bending moment at midlength of each specimen. In addition, failure modes of the tested specimens are also recorded in the table, in which F represents flexural failure and SS stands for shear splitting failure. Figs. 3(a and b) show two photographs of the tested specimens exhibiting shear splitting failure and flexural failure, respectively. More detailed observations of the mechanical behavior of the tested specimens are presented in the following sections.
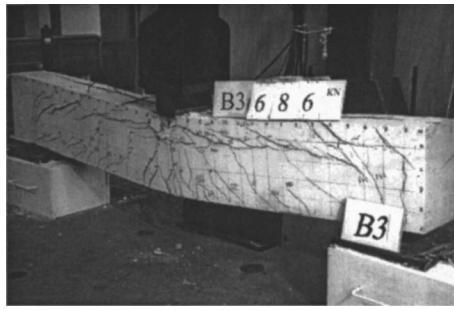
Load–Deflection Curves

Fig. 4 shows two typical load–deflection curves of the tested specimens. The curve shown in Fig. 4(a) represents the load–deflection relationship of the specimens with shear splitting failure. Observations from the tests indicated that, at point B_s (point of shear splitting failure), the applied load dropped suddenly when the horizontal cracks appeared along the interface of steel flange and concrete. A possible reason for the load drop is the appearance of the horizontal cracks that resulted in a reduction of the effective compressive area of the concrete. After the load

Table 3. Test Strength and Failure Mode of Composite Beams

Specimen designation	Bond condition	Test Strength		Failure[a] mode
		V_{test} (kN)	M_{test} (kN m)	
Specimens with flange width ratio=0.67 (f_f=200 mm)				
B1-20-S	Shear stud	365.5	548.2	F
B2-20-G	Grease	327.4	491.1	SS
B3-20-N	Natural bond	339.1	508.7	SS
B4-20-N	Natural bond	354.5	531.7	SS
B5-20-N	Natural bond	312.7	469.1	SS
B6-20-N	Natural bond	244.1	366.2	SS
Specimens with flange width ratio=0.50 (b_f=150 mm)				
B7-15-S	Shear stud	312.3	468.4	F
B8-15-G	Grease	289.3	434.0	F
B9-15-N	Natural bond	317.5	476.3	F
Ordinary RC beam				
B10-RC	—	130.0	195.0	F

[a]SS=shear splitting failure, shown in Fig. 3(a). F=flexural failure, shown in Fig. 3(b).

1188 / JOURNAL OF STRUCTURAL ENGINEERING / SEPTEMBER 2002

(a) Shear splitting failure
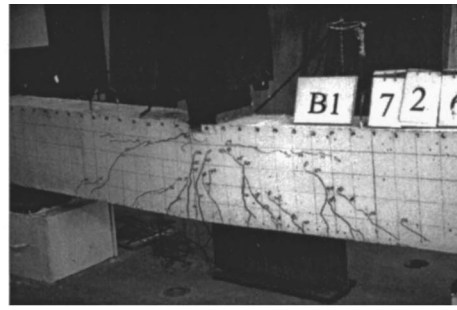
(b) Flexural failure

Fig. 3. Failure modes of concrete encased steel beams

dropped from point B_s to C_s (point of strength recovery), the load–deflection curve was observed to rise up again. It is interesting to note that the gradual increase of strength from point C_s to D_s (point of ultimate capacity) is mainly a contribution of the flexural resistance of the steel shape.

The curve shown in Fig. 4(b) represents the load–deflection relationship of the specimens with flexural failure. In this figure, the load–deflection curve of a composite beam can be divided into two stages. One is from point A_F to B_F (point of stiffness softening), the other is from point B_F to C_F (point of ultimate capacity). Before the load reached point B_F, the specimen exhibited elastic behavior. However, the stiffness reduction caused by the cracking of concrete became apparent from point B_F to C_F. Evidence from the strain gauge readings showed that part of the steel section had come into the plastic range at this stage. After point C_F, concrete crushing and buckling of rebars on the compressive side occurred, and the specimen failed with the fracture of rebars on the tension side.

Crack Patterns

Also shown in Fig. 4 is the sequence of the development of cracks for each failure mode. The development of the cracks for the specimens with shear splitting failure is shown in Fig. 4(a). The flexural cracks appeared first at the bottom of specimen from point A_S to B_S shown on the load–deflection curve. As the load increased, 45° flexural-shear cracks formed near both ends of the specimen. When the load reached point B_S, the horizontal cracks along the top steel flange appeared. From point B_S to C_S, the horizontal cracks extended from the center to both ends of the
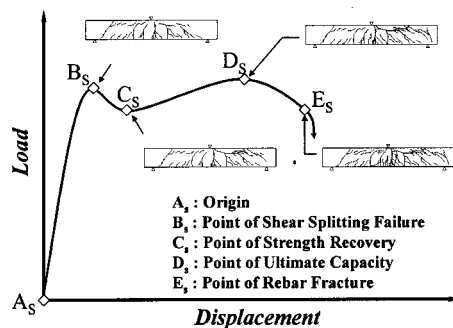
specimen. Finally, the horizontal cracks connected with the flexural-shear cracks during the stage from point C_S to D_S.

Fig. 4(b) shows the sequence of the development of cracks for the specimens with flexural failure. It was observed that, from point A_F to B_F shown on the load–deflection curve, flexural cracks appeared at the bottom of specimen. When the load increased from point B_F to C_F, the cracks extended from the bottom of the specimen to the loading point. Finally, many flexural cracks formed near the midlength of the specimen and failure occurred during the stage form point C_F to D_F.
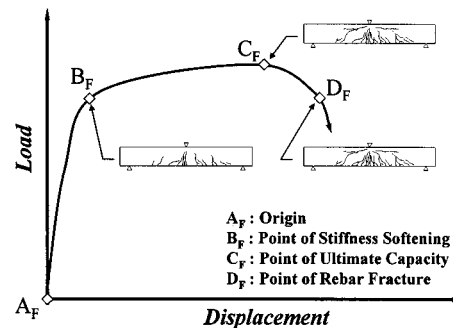
Figs. 3(a and b) show two photographs of the composite beams with shear splitting failure and flexural failure, respectively. Significant crack and spalling of concrete in the compressive area of the specimen were observed from the specimen with shear splitting failure along the top steel flange. In contrast, for the specimen with flexural failure, concrete crushing occurred mainly near the midlength of the specimen. Figs. 5(a and b) show an apparent deformation of a stirrup and a slip between the steel flange and concrete in specimens with shear splitting failure. These figures indicated that full composite action between the steel flange and concrete was not achieved in these specimens.

Influences of Steel Flange Width Ratio and Bond Conditions

Fig. 6 shows the load–deflection curves of the specimens with the larger steel flange width ratio of 0.67. It is noted that all specimens were subjected to shear splitting failure except Specimen B1 that was designed with shear studs on its upper steel flange.


A_s : Origin
B_s : Point of Shear Splitting Failure
C_s : Point of Strength Recovery
D_s : Point of Ultimate Capacity
E_s : Point of Rebar Fracture

A_F : Origin
B_F : Point of Stiffness Softening
C_F : Point of Ultimate Capacity
D_F : Point of Rebar Fracture

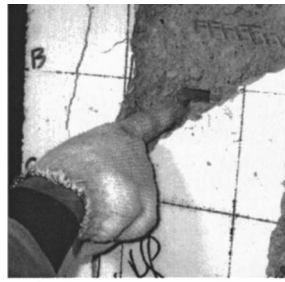(a) Specimens with shear splitting failure

(b) Specimens with flexural failure

Fig. 4. Illustration of load–deflection curve and development of cracks
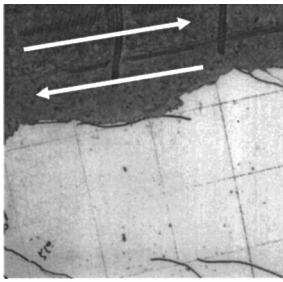
(a) Deformation of stirrup **(b) Slip of steel flange**

Fig. 5. Relative slip between steel flange and concrete in specimen with shear splitting failure

As a comparison, Fig. 7 shows the load–deflection curves of the specimens with the smaller steel flange width ratio of 0.5. It is interesting to note that only flexural failure was observed for the specimens shown in Fig. 7. The main difference between these two groups of specimens shown in Figs. 6 and 7 is the steel flange width ratio. By comparing the load–deflection curves of Figs. 6 and 7 and the observed failure modes of the specimens recorded in Table 3, it becomes obvious that the steel flange width ratio plays a significant role in the shear splitting failure of the concrete encased steel beams. The test results indicated that the shear splitting failure occurred when the steel flange width ratio of a composite beam reached 0.67.

In addition, as shown in Fig. 6, a comparison between the load–deflection curve of Specimen B1 (with shear studs) and the rest of the curves of specimens without shear studs reveals that the application of shear studs in the composite beam has a posi-

tive effect in preventing the shear splitting failure for a beam with large steel flange ratio. This explains why all specimens with the steel flange ratio of 0.67 suffered from shear splitting failure except Specimen B1.

For the specimens subjected to flexural failure, the influence of bond condition between steel flange and concrete on the behavior of the composite beams can be studied from Table 3 and Fig. 7. It is noted that Specimens B7, B8, and B9 were designed with different bond conditions (denoted as S, G, or N). Evidence from the test strengths and the load–deflection curves of these specimens reveals that:

1. By comparing the test strengths of Specimens B7 (with studs) and B9 (natural bond) shown in Table 3, it is found that the presence of shear studs has almost no influence on the ultimate strength of the composite beams. Nevertheless, from Fig. 7, Specimen B7 showed slightly better ductility than that of Specimen B9.
2. By comparing the test strengths of Specimen B8 (greased) to Specimens B7 and B9, it is observed that the ultimate strength of Specimen B8 is about 10% smaller than the strengths of the other two specimens. The reduced strength for Specimen B8 appears to result from the layer of grease breaking the bond between the steel shape and the concrete. The total deflection of the greased specimen is also found to be somewhat smaller than that of Specimens B7 and B9, as indicated by Fig. 7.

Proposed Design Method to Prevent Shear Splitting Failure

Experiments performed in this study have shown that the shear splitting failure is possible and may occur before a composite
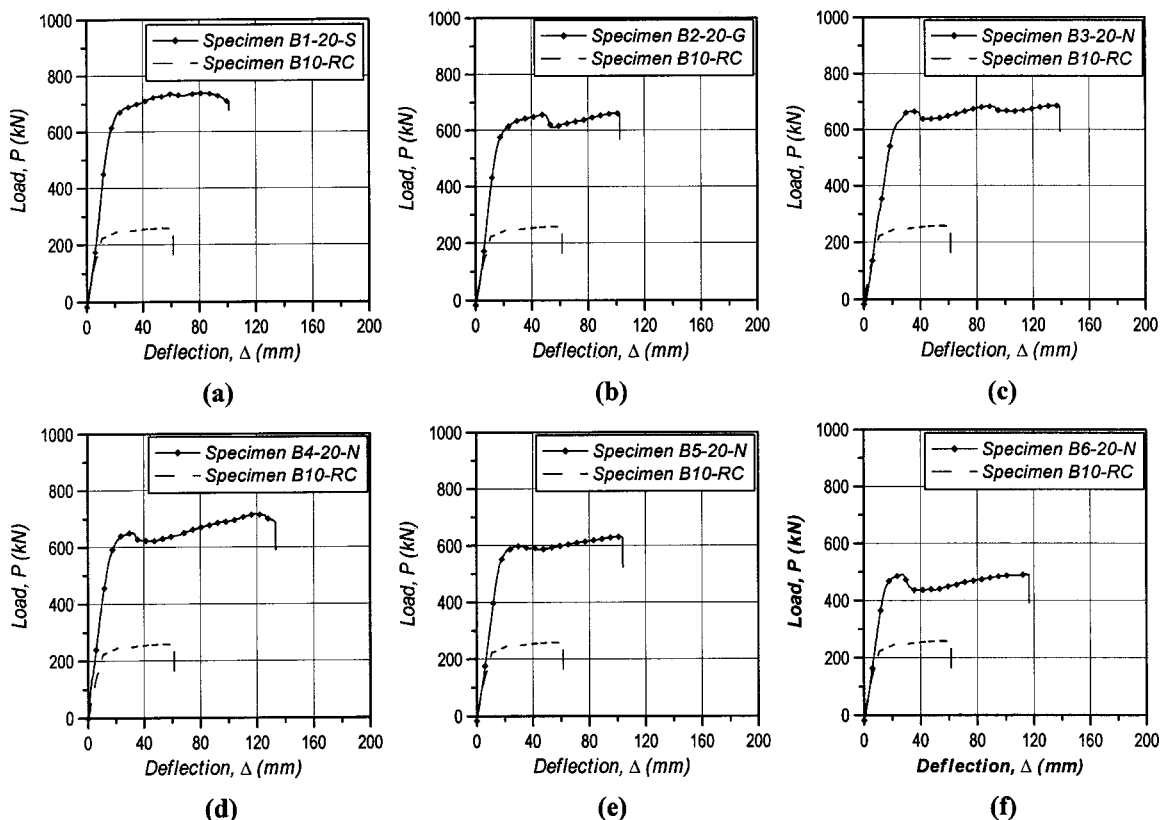

Fig. 6. Load–deflection curves of specimens with steel flange width ratio of 0.67
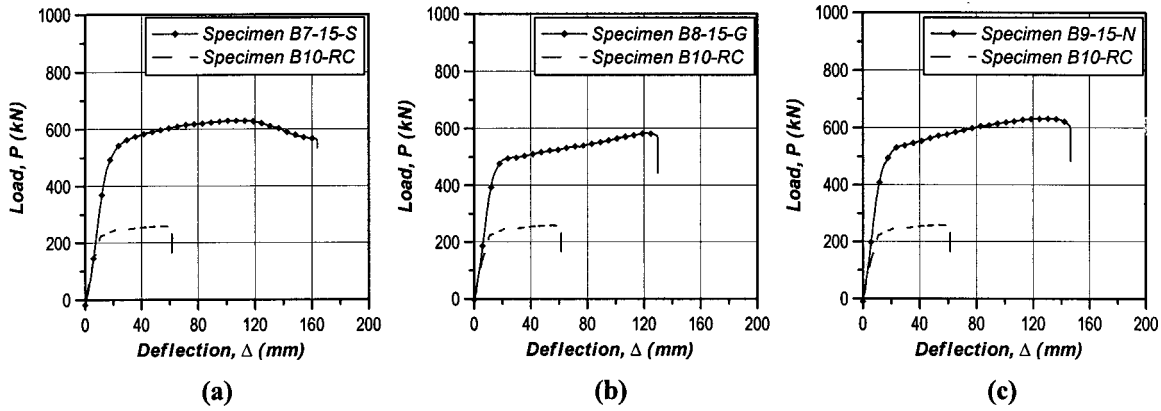
Fig. 7. Load–deflection curves of specimens with steel flange width ratio of 0.5

beam reaches its ultimate flexural capacity. To prevent this type of failure, a composite beam should be designed with sufficient internal shear splitting resisting capacity $(V_{SS})_n$ to resist the horizontal shear force V_h transferred between the interface of steel flange and concrete. To meet this condition, it will require that

$$(V_{SS})_n \geqslant V_h \qquad (1)$$

Calculation of Horizontal Shear Force

To determine the magnitude of the horizontal shear force V_h, the concept of plastic stress distribution on composite section used in the AISC LRFD specification (AISC 1999) is adopted in this study. The basic assumptions of the plastic stress distribution include:

1. A uniformly distributed steel stress of F_{ys}, yielding stress of steel section, is assumed throughout the tensile and compressive zones;
2. A concrete stress of $0.85f'_c$ is assumed to be uniformly distributed throughout the compressive zone, and the concrete tensile strength is neglected;
3. A tensile strength of F_{yr}, yielding strength of reinforcing bar, is assumed in adequately developed longitudinal reinforcing bars in both tension and compressive zones;
4. The net tensile force is equal to the net compressive force in a composite section.

As shown in Fig. 8, the location of the plastic neutral axis (PNA) of a composite beam based on the above assumptions may fall into one of the two general cases: (1) PNA within the compressive concrete portion; and (2) PNA within the steel section. If the PNA is located in the compressive concrete portion, the mag-

nitude of the compressive force $0.85f'_cBd_f$ will be larger than the tensile force A_sF_{ys}. On the contrary, $0.85f'_cBd_f$ will be smaller than A_sF_{ys} if the PNA is located in the steel section. Therefore, the horizontal shear force along the interface of steel flange and concrete can be expressed as

$$V_h = A_sF_{ys} + A'_rF_{yr}$$

when

$$0.85f'_cBd_f > A_sF_{ys} \qquad (2a)$$

or

$$V_h = 0.85f'_cBd_f + A'_rF_{yr}$$

when

$$0.85f'_cBd_f \leqslant A_sF_{ys} \qquad (2b)$$

in which f'_c = concrete compressive strength; B = width of the composite beam; d_f = concrete cover thickness shown in Fig. 8; A'_r = area of rebars in compressive zone; and A_s = area of the steel section.

If the horizontal shear force, V_h, determined from Eqs. (2a) or (2b) is larger than the shear splitting resisting capacity $(V_{SS})_n$ of the composite beam, the shear splitting failure mode will be dominant.

Prediction of Shear Splitting Resisting Capacity

To determine the shear splitting resisting capacity $(V_{SS})_n$, a shear-friction analogy of an ordinary reinforced concrete member
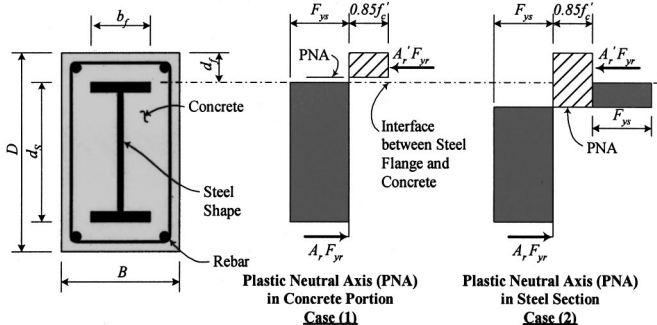

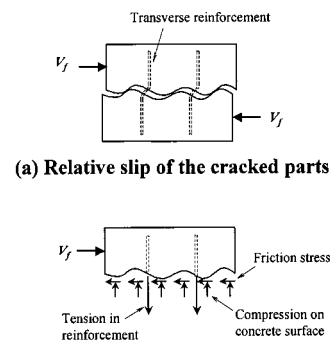**Fig. 8.** Plastic stress distribution on composite beam section

(a) Relative slip of the cracked parts

(b) Relation between compression on concrete and tension in reinforcement

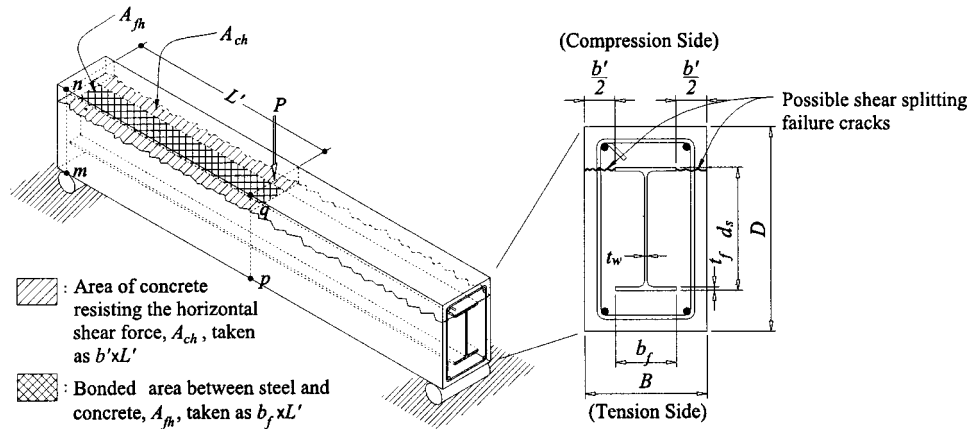**Fig. 9.** Shear-friction analogy (ACI-ASCE committee 426 1973)

Fig. 10. Proposed analytical model for shear splitting failure along interface between steel flange and concrete

suggested by ACI–ASCE Committee 426 (1973) is utilized. As shown in Fig. 9(a), when a horizontal shear force is applied to a resisting capacity (RC) specimen, the relative slip of the cracked parts causes a separation of the cracked surfaces. If there is a transverse reinforcement across the crack, it is elongated by the separation of the surfaces and hence is stressed in tension. For equilibrium, compressive stresses acting on the concrete surface are needed as shown in Fig. 9(b). It is observed that the shear force is transmitted across the cracked surface in the following ways: (1) friction resulting from the compressive stress acting on the cracked surfaces, and (2) interlock of aggregate protrusions on the cracked surfaces combined with dowel action of the reinforcement crossing the surface.

Test results on the shear-friction behavior of RC members presented by Hofbeck et al. (1969) and Mattock and Hawkins (1972) indicated that the shear friction strength of a cracked surface with transverse reinforcements perpendicular to the shear plane is given as

$$V_f = \mu_f A_{vf} F_{yh} + K_1 A_c \leq 0.3 f'_c A_c \qquad (3)$$

in which μ_f= shear friction coefficient, taken as 0.8 for concrete sliding on concrete; A_{vf}= area of transverse reinforcements crossing the shear plane; F_{yh}= yield stress of transverse reinforcement; K_1= empirical constant, taken as 2.8 MPa for normal weight concrete; and A_c= area of concrete surface resisting shear friction.

The first term in Eq. (3) represents the friction force; and the second term denotes the shear transferred by shearing off surface protrusions and by dowel action.

Due to the presence of the steel shape in a composite beam, the shear-friction analogy of a concrete encased steel beam is somewhat different from that of an ordinary RC member. Thus, both the shear-friction model of Fig. 9 and Eq. (3) need to be modified so that they can be used to determine the shear splitting capacity of a composite beam. Details of the modifications are as follows.

Figs. 10 and 11 illustrate the proposed new analytical model for the behavior of a composite beam subjected to shear splitting failure. Fig. 10 depicts the shear splitting cracks along the interfaces of steel flange and concrete, and Fig. 11 displays the free-body diagram along the cracked plane in the horizontal shear transfer region (between the point of maximum moment and the point of zero moment). From Figs. 10 and 11, the shear splitting resisting capacity in the horizontal shear transfer region $(V_{SS})_n$ can be taken as

$$(V_{SS})_n = \mu_f A_{vf} F_{yh} + K_1 A_{ch} + f_s A_{fh} \qquad (4)$$

in which A_{ch}= area of concrete resisting the horizontal shear friction force within a distance L', taken as $L' \times b'$; L'= distance between the points of maximum moment and zero moment; and b'= effective width of the concrete section to resist shear splitting
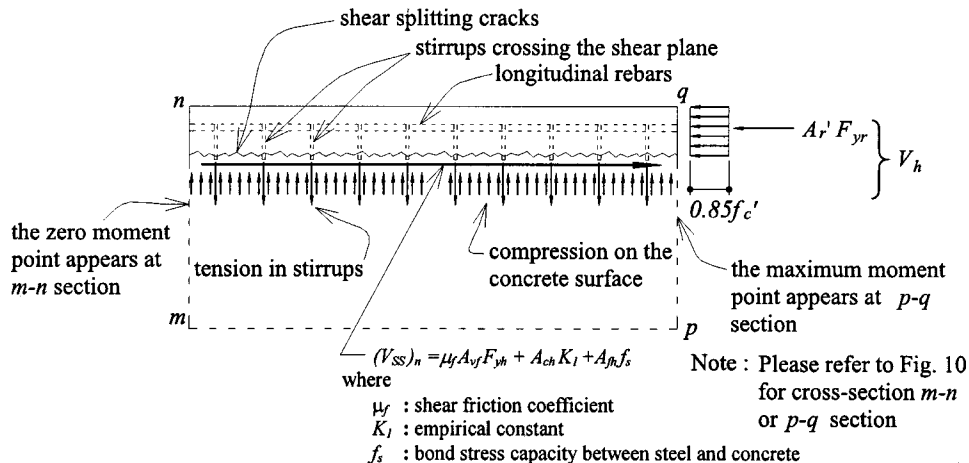

Fig. 11. Shear splitting resisting capacity $(V_{SS})_n$ along cracked plane

Table 4. Failure Modes Predicted by Proposed Approach

Specimen designation	V_h (kN)	$(V_{SS})_n$ (kN)	Predicted[a] failure mode	Observed[b] failure mode
B1-20-S	1325.0	1855.2	F	F
B2-20-G	NA	NA	NA	SS
B3-20-N	1317.1	1147.9	SS	SS
B4-20-N	1322.3	1147.9	SS	SS
B5-20-N	1335.5	1187.8	SS	SS
B6-20-N	1335.5	1210.7	SS	SS
B7-15-S	1288.7	2063.5	F	F
B8-15-G	NA	NA	NA	F
B9-15-N	1306.6	1323.4	F	F

[a]SS = shear splitting failure if $(V_{SS})_n$ is smaller than V_h, F = flexural failure if $(V_{SS})_n$ is larger than V_h, and NA = not applicable.
[b]Failure modes observed from tests.

failure, taken as $(B-b_f)$; b_f = width of the steel flange; f_s = bond stress between steel flange and concrete; A_{fh} = area along the interface between steel flange and concrete within a distance L', taken as $L' \times b_f$.

In Eq. (4), the first two terms denote the contribution similar to that from the shear-friction analogy of an ordinary reinforced concrete member [Eq. (3)] and the last term is the contribution of bond stress f_s between steel flange and concrete. Roeder et al. (1999) investigated the magnitude of the bond stress between steel and concrete. For natural bond condition, their experimental results indicated that the bond stress can be determined by using the following equation:

$$f_s = 1.256 - 9.544\rho \tag{5}$$

in which ρ = ratio of steel section area to gross section area. In this study, the above equation proposed by Roeder et al. (1999) is adopted and used in Eq. (4) to determine the shear splitting resisting capacity of a composite beam with natural bond condition.

For a composite beam with shear studs on the steel flange, the recommendation proposed by Roeder et al. (1999) is also used to determine its shear splitting resisting capacity $(V_{SS})_n$. It is recommended that the load transferred between steel and concrete shall be calculated either entirely by bond or entirely by shear studs and not by any combination of the two. Therefore, the shear splitting resisting capacity of a composite beam with shear studs shall be the larger of Eq. (4) and the following equation:

$$(V_{SS})_n = \mu_f A_{vf} F_{yh} + K_1 A_{ch} + N \times Q_n \tag{6}$$

in which N = total numbers of shear stud within a distance L'; and Q_n = nominal strength of one shear stud. In this study Q_n is determined by using Eq. (I5-1) given in the AISC-LRFD specification (1999).

Verification of Proposed Approach

Table 4 shows the predicted failure modes of the tested specimens based on the proposed approach. In this table, the horizontal shear force V_h and the shear splitting resisting capacity $(V_{SS})_n$ of a composite beam are calculated by using the proposed Eqs. (2), (4), and (6). Both of the predicted failure modes and the observed failure modes of the tested specimens are shown in the table.

For specimens with natural bond condition or shear studs, comparisons between the calculated values of V_h and $(V_{SS})_n$ indicate that the shear splitting failure mode is dominant for Specimens B3, B4, B5, and B6 because the calculated horizontal shear

forces are larger than the shear splitting resisting capacities. On the contrary, flexural failure mode is dominant for Specimens B1, B7, and B9 because the calculated horizontal shear forces are smaller than the shear splitting resisting capacities. It is noted that all of the predicted failure modes matched observed failure modes from tests. This indicates that the proposed Eqs. (2), (4), and (6) give satisfactory predictions of the failure mode of the composite beams with natural bond condition or shear studs.

In Table 4, the shear splitting resisting capacities of the greased specimens are not calculated due to the uncertainty of the bond stress f_s. In addition, the horizontal shear forces of the greased specimens are not included because the assumption of full interaction between steel and concrete cannot be satisfied.

Design Application

Based on the above analysis, it is the writers' observation that the shear splitting failure of a naturally bonded composite beam can be prevented if the stirrups are adequately designed to make the beam develop sufficient shear splitting capacity for resisting the horizontal shear force along the interface of steel flange and concrete. To evaluate the amount of the stirrups needed, substituting Eq. (4) into Eq. (1) leads to

$$\mu_f A_{vf} F_{yh} + K_1 A_{ch} + f_s A_{fh} \geq V_h \tag{7}$$

Eq. (7) can be expressed as

$$\mu_f n A_v F_{yh} + (K_1 b' + f_s b_f) L' \geq V_h \tag{8}$$

in which n = number of stirrups crossing the interface of steel flange and concrete, taken as L'/S, where S = stirrup spacing, and A_v = cross-sectional area of both legs of one stirrup. To avoid the shear splitting failure, it will be necessary to satisfy

$$\frac{A_v}{S} \geq \left(\frac{V_h}{\mu_f F_{yh} L'} - \frac{K_1 b' + f_s b_f}{\mu_f F_{yh}} \right) \tag{9}$$

Thus, the shear splitting resisting capacity of a naturally bonded composite beam will be sufficient to resist the horizontal shear force if the amount of stirrups satisfies the requirement of Eq. (9).

Summary and Conclusions

The major results obtained from this research are summarized as follows:
1. Nine full-scale specimens were designed, fabricated, and tested to investigate the flexural and shear behavior of concrete encased steel beams. The test strength, load–deflection curve, crack pattern, and failure mode of each specimen were recorded and studied carefully.
2. Based on the crack patterns of the tested specimens, the failure modes of the concrete encased steel beams are classified into two different types which are the flexural failure mode and the shear splitting failure mode.
3. Shear splitting failure resulted in significant horizontal cracks of concrete along the steel flange and caused a sudden drop of load before the beam reached its ultimate capacity. However, due to the presence of the steel shape within the specimen, the composite beam could still sustain further loading until it reached its ultimate strength.
4. For the specimens with the larger steel flange width ratio of 0.67, shear splitting failure was observed along the interface between steel flange and concrete. On the contrary, for the specimens with the smaller steel flange width ratio of 0.5, flexural failure was observed from the tests.

5.   Evidence from the test results indicated that the application of shear studs on the steel flange had a positive effect on preventing the shear splitting failure for composite beams with large steel flange ratio. However, for the specimens failed in flexure, the addition of shear studs contributed little to the ultimate flexural capacity of the composite beams.

6.   In addition to the experimental work, an analytical study is performed to derive a new set of equations to determine the magnitudes of the horizontal shear force and the shear splitting resisting capacity of the concrete encased steel beams.

7.   Based on the derived equations, the failure mode of a concrete encased steel beam can be predicted. Furthermore, a new formula for the design of the stirrups is proposed to prevent the shear splitting failure of naturally bonded composite beams.

Acknowledgments

Notation

The following symbols are used in this paper:

A_c = area of concrete surface resisting shear friction;

A_{ch} = area of concrete resisting horizontal shear friction force within distance L';

A_{fh} = area along interface between steel flange and concrete within distance L';

A_r' = area of reinforcing bars in compressive zone;

A_s = area of steel section;

A_v = cross-sectional area of both legs of one stirrup;

A_{vf} = area of stirrups crossing shear plane;

B = width of composite beam;

b' = effective width of concrete section to resist shear splitting failure;

b_f = width of steel flange;

d_f = concrete cover thickness;

F_{ys}, F_{yr}, F_{yh}

= yielding stress of steel section, reinforcing bar, and stirrup, respectively;

f_c' = concrete compressive strength;

f_s = bond stress between steel flange and concrete;

f_y, f_u = yielding stress and tensile strength of steel shape (or reinforcing bar or stirrup), respectively;

K_1 = empirical constant, taken as 2.8 MPa for normal weight concrete;

L' = distance between points of maximum moment and zero moment;

N = numbers of shear stud within distance L';

n = numbers of stirrups crossing interface of steel flange and concrete;

Q_n = nominal strength of one shear stud;

S = stirrup spacing;

V_f = shear friction strength of cracked surface with stirrups perpendicular to shear plane;

V_h = horizontal shear force;

$(V_{SS})_n$ = shear splitting resisting capacity of concrete encased steel beam;

μ_f = shear friction coefficient, taken as 0.8 for concrete sliding on concrete; and

ρ = ratio of steel section area to gross section area.

References

ACI (1999). ''Building code requirements for structural concrete (ACI 318-99) and commentary (ACI 318R-99)'' *ACI 318-99*, Farmington Hills, Mich.

ACI-ASCE Committee 426 (1973). ''The shear strength of reinforced concrete members.'' *J. Struct. Div. ASCE,* 99(ST6), 1148–1157.

AIJ (2001). ''Standards for structural calculation of steel reinforced concrete structures.'' Architectural Institute of Japan, Tokyo.

AISC (1999). ''Load and resistance factor design specification for structural steel buildings.'' American Institute of Steel Construction, Chicago.

ASTM (1991a). ''Standard methods for compression testing of cylindrical concrete specimens.'' *C39-72*, Philadelphia.

ASTM (1991b). ''Standard methods for tension testing of metallic materials.'' *E8-91*, Philadelphia.

BSSC (1997). ''NEHRP recommended provisions for the development of seismic regulations for new buildings and other structures.'' *National Earthquake Hazards Reduction Program*, Building Seismic Safety Council, Washington, D.C.

El-Tawil, S., and Deierlein, G. G. (1999). ''Strength and ductility of concrete encased composite columns.'' *J. Struct. Eng.,* 125(9), 1009–1019.

El-Tawil, S., Sanz-Picòn, C. F., and Deierlein, G. G. (1995). ''Evaluation of ACI 318 and AISC (LRFD) strength provisions for composite beam-columns.'' *J. Constr. Steel Res.,* 34, 103–123.

Furlong, R. W. (1968). ''Design of steel-encased concrete beam-columns,'' *J. Struct. Eng.,* 94(1), 267–281.

Hofbeck, J. A., Ibrahim, I. O., and Mattock, A. H. (1969). ''Shear transfer in reinforced concrete.'' *ACI J.,* 66(2), 119–128.

Johnson, R. P., and May, I. M. (1978). ''Tests on restrained composite columns.'' *Structural Engineers,* London, 56B(2), June, 21–28.

Mattock, A. H., and Hawkins, N. M. (1972). ''Shear transfer in reinforced concrete—recent research.'' *J. Prestressed Concr. Inst.,* 17(2), 55–75.

Mirza, S. A. (1989). ''Parametric study of composite column strength variability,'' *J. Constr. Steel. Res.,* 14(2), 121–137.

Mirza, S. A., Hyttinen, V., and Hyttinen, E. (1996). ''Physical tests and analyses of composite steel-concrete beam-columns.'' *J. Struct. Eng.,* 122(11), 1317–1326.

Muñoz, P. R., and Hsu, C.-T. T. (1997a). ''Behavior of biaxial loaded concrete-encased composite columns.'' *J. Struct. Eng.,* 123(9), 1163–1171.

Muñoz, P. R., and Hsu, C.-T. T. (1997b). ''Biaxial loaded concrete-encased composite columns: design equation.'' *J. Struct. Eng.,* 123(12), 1576–1585.

Naka, T., Morita, K., and Tachibana, M. (1977). ''Strength and hysteretic characteristics of steel-reinforced concrete columns (Part 2).'' *Trans. AIJ,* 250, 47–58.

Procter, A. N. (1967). ''Tests on stability of concrete encased I-beams.'' *Consulting Engineer,* London, England, Feb., 56–58, Mar., 59–61.

Ricles, J. M., and Paboojian, S. D. (1994). ''Seismic performance of steel-encased composite columns.'' *J. Struct. Eng.,* 120(8), 2474–2494.

Roeder, C. W., Chmielowski, R., and Brown, C. B. (1999). ''Shear connector requirements for embedded steel sections.'' *J. Struct. Eng.,* 125(2), 142–151.

Wakabayashi, M. (1987). ''A historical study of research on composite construction in Japan.'' *Proc., Conf. Composite Construction in Steel and Concrete*, ASCE, New York, 400–427.